Journal of Nanobiotechnology

RESEARCH

Open Access

Optimal development of apoptotic cells-mimicking liposomes targeting macrophages

Li Zhang[1†], Yujiao Li[2†], Xing Liu[3†], Xiaolu He[2], Jieyu Zhang[2], Jun Zhou[2], Youbei Qiao[4], Hong Wu[4*], Fangfang Sun[1*] and Qing Zhou[2*]

Abstract

Macrophages are multifunctional innate immune cells that play indispensable roles in homeostasis, tissue repair, and immune regulation. However, dysregulated activation of macrophages is implicated in the pathogenesis of various human disorders, making them a potential target for treatment. Through the expression of pattern recognition and scavenger receptors, macrophages exhibit selective uptake of pathogens and apoptotic cells. Consequently, the utilization of drug carriers that mimic pathogenic or apoptotic signals shows potential for targeted delivery to macrophages. In this study, a series of mannosylated or/and phosphatidylserine (PS) -presenting liposomes were developed to target macrophages via the design of experiment (DoE) strategy and the trial-and-error (TaE) approach. The optimal molar ratio for the liposome formulation was DOPC: DSPS: Chol: PEG-PE = 20:60:20:2 based on the results of cellular uptake and cytotoxicity evaluation on RAW 264.7 and THP-1 in vitro. Results from in vivo distribution showed that, in the DSS-induced colitis model and collagen II-induced rheumatoid arthritis model, PS-presenting liposomes (PS-Lipo) showed the highest accumulation in intestine and paws respectively, which holds promising potential for macrophage target therapy since macrophages are abundant at inflammatory sites and contribute to the progression of corresponding diseases. Organs such as the heart, liver, spleen, lung, and kidney did not exhibit histological alterations such as inflammation or necrosis when exposed to PC-presenting liposomes (PC-Lipo) or PS-Lipo. In addition, liposomes demonstrated hemobiocompatibility and no toxicity to liver or kidney for circulation and did not induce metabolic injury in the animals. Thus, the well-designed PS-Lipo demonstrated the most potential for macrophage target therapy.

Keywords Macrophage, Liposome, Phosphatidylserine, Mannosylated, Design of experiment

†Li Zhang, Yujiao Li and Xing Liu contributed equally to this work.

*Correspondence:
Hong Wu
wuhong@fmmu.edu.cn
Fangfang Sun
sff0517@163.com
Qing Zhou
qingchou0504@163.com

[1]Department of Prosthodontics, Nanjing Stomatological Hospital, Affiliated Hospital of Medical School,Institute of Stomatology,Nanjing University, Nanjing 210002, China
[2]Department of Clinical Pharmacy, Jinling Hospital, Medical School of Nanjing University, Nanjing 210002, China
[3]Department of Infectious Disease and Liver Disease, the Second Hospital of Nanjing, Nanjing University of Chinese Medicine, Nanjing 210003, China
[4]Department of Medicinal Chemistry and Pharmaceutical Analysis, School of Pharmacy, Air Force Medical University, Xi'an 710032, China

Introduction

Macrophages are multifunctional innate immune cells that are present in all body tissues and play indispensable roles in host defense, homeostasis, tissue repair, and immune regulation [1–3]. They are derived from monocytes, which are produced in the bone marrow and circulate in the blood while entering the tissues, monocytes differentiate into macrophages. Resident macrophages display remarkable plasticity and can change their functional state in response to changes in physiology as well as challenges from the outside [4, 5]. Unfortunately, in many cases, macrophages are inappropriately activated, and consequently, their homeostatic and reparative functions would be subverted, resulting in a causal association between dysfunctional macrophages and disease states, such as acute/chronic inflammation, cardiovascular disease, cancer, chronic wound, and neurodegenerative diseases [6, 7]. Due to their wide-ranging involvement in the pathogenesis of various human diseases, macrophages are considered to be an extremely attractive and relevant therapeutic target. The aim for targeting and modulating macrophages holds promising potential for the treatment of corresponding diseases, in which the crucial concern to be addressed is the development of ideal formulations for targeted delivery to macrophages.

The past few decades have witnessed significant progress in nanotechnology field and have gained increasing interest in the development of functional nanomedicines for the diagnosis, imaging, and therapy of many diseases and conditions [8, 9]. Nanoparticles (NPs) are key components of nanomedicine. A wide variety of nanomaterials have been explored to construct NPs, including lipids, polymers, proteins, nucleic acids, inorganic nanomaterials, etc [10, 11]. Currently, lipid-based nanoparticles (LNPs) have been propelled in the spotlight of therapeutic platforms due to the success of the COVID-19 mRNA vaccines (mRNA-1273 and BNT162b2), in which LNPs played a key role in effectively protecting and transporting mRNA to cells [12–14]. Liposomes, an early version of LNPs, are considered one of the most flexible and successful nanomedicine delivery platforms, which can encapsulate a wide range of drugs, including small molecules, peptides, proteins, and nucleic acids [15, 16]. Furthermore, the liposomal surface can be modified with various ligands, including antibodies, peptides, and carbohydrates, to enhance targeting and uptake by specific cells. Several liposomal drugs have been approved and are available for the treatment of various diseases [17].

Phosphatidylserine (PS), a crucial phospholipid resident in the cell membrane, extends its influence beyond the realm of structural integrity. One of its distinctive functions involves signaling cellular events, particularly in the intricate process of apoptosis, where cells undergo programmed self-destruction. The externalization of PS is a hallmark of apoptotic cells, serving as a recognition signal for phagocytic clearance, often mediated by macrophages [18–20]. In the orchestration of apoptotic pathways, PS translocation from the primarily inner leaflet to the outer leaflet of the cell membrane acts as an "eat me" signal, facilitating the prompt recognition and engulfment of dying cells by macrophages. This process not only ensures the efficient removal of compromised or unnecessary cells but also plays a crucial role in immune regulation and tissue homeostasis. This unique property of macrophages can be exploited to selectively target liposomes modified with PS to sites of inflammation, infection, or other pathological conditions where macrophages are abundant [21]. In addition, mannose receptors, abundantly expressed on the surface of macrophages, are specialized in recognizing and binding to mannose-containing ligands. This physiological characteristic has inspired researchers to leverage mannose-modification as a means to create nanoparticles with a heightened affinity for macrophages. By coating nanoparticles with mannose or incorporating mannose moieties into their structure, these modified particles gain the ability to engage with and be selectively internalized by macrophages, presenting a targeted approach for drug delivery [22–24].

In this study, mannosylated or/and PS lipid-presenting liposomes have been developed to target macrophages (Scheme 1A). Design of experiment (DoE) strategy and trial-and-error (TaE) approach were used to identify the optimal liposomal formulation by considering the size, surface charge, macrophage targeting efficiency, and minimizing cytotoxicity. The transition from in vitro screening to in vivo validation represents a critical phase in the development of liposomal formulations for targeted therapy. Thus, following the in vitro screening process to identify the optimal liposomal formulation, three well-established murine inflammatory models were used to validate the targeting specificity of the optimized liposomal formulation at inflammation sites, within which macrophages were abundant and contribute to the progression of corresponding diseases, through the in vivo biodistribution imaging (Scheme 1B). In addition, the in vivo biocompatibility of the prepared liposomes was evaluated. Insights gained from this study are expected to contribute significantly to the development of targeted therapeutic strategies for a variety of macrophage-associated diseases.

Results and discussion

DoE strategy optimized the ratio of individual lipids within liposomes

The pursuit of designing efficient drug delivery systems has fueled the exploration of various formulation strategies to enhance the performance of drug carriers. Among

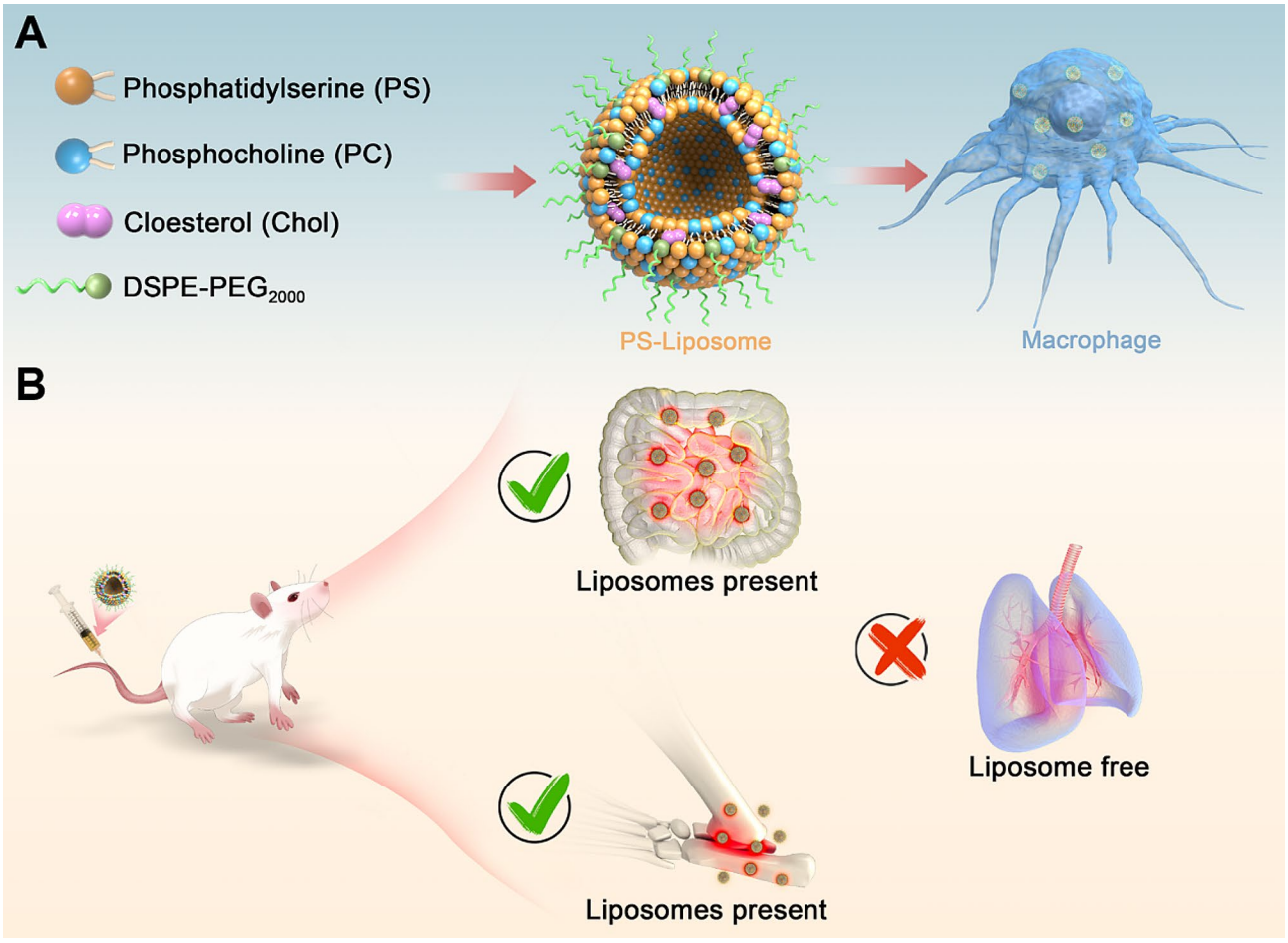

Scheme 1 (**A**) Schematic illustration of the formulation of PS-presenting liposomes and targeting delivery to macrophages. (**B**) In vivo validation of the targeting ability of PS-presenting liposomes in three murine inflammatory models, showing specific targeting to inflamed sites in DSS-induced colitis and collagen II-induced rheumatoid arthritis models, but not in that of LPS-induced lung inflammation model

these strategies, the DoE strategy has emerged as a powerful and systematic approach for optimizing the formulation of liposomes [25, 26]. As a versatile statistical tool, DoE enables a structured exploration of the multifaceted parameter space involved in liposomal development. In this study, pathogenic or apoptotic signals mimicking liposomes were developed and explored to achieve maximizing macrophage targeting while minimizing cytotoxicity. Mannosylated or/and phosphatidylserine (PS) -presenting liposomes were developed to mimic pathogenic and apoptotic signals. Initially, 1,2-dipalmitoyl-sn-glycero-3-phospho-L-serine (DPPS) was selected to prepare PS-presenting liposomes, and mannose (Man) -conjugated 1,2-distearoyl-sn-glycero-3-phosphoethanolamine-N-[methoxy(polyethylene glycol)-2000 (DSPE-PEG) was synthesized to realize mannosylation. The synthesis of Man-PEG-DSPE was illustrated in Figure S1A, and the product was characterized by ^{1}H NMR. The ^{1}H-NMR spectrum of DSPE-PEG and Man-PEG-DSPE are shown in Figure S1B and S1C respectively. As shown in Figure S1C, the signals at 3.5–4.3 ppm represented the phenyl and hydroxyl groups in 4-aminophenyl α-D-mannopyranoside, indicating the successful reaction between the amino group and the NHS group in DSPE-PEG-NHS.

Firstly, a series of liposomes with 17 formulations (Library A) were generated by the DoE strategy by varying the molar ratio of the compositions including DPPS, 1,2-distearoyl-sn-glycero-3-phosphocholine (DSPC), cholesterol (Chol), and Man-PEG-DSPE (Fig. 1A and B). The liposomes were highly uniform with particle size ranging between 80 and 100 nm, and a polydispersity index (PDI) consistently below 0.2 (Fig. 1C). As the ratio of DPPS increased, zeta potential decreased, whereas increased PEG content resulted in formulations approaching neutral zeta potentials (Fig. 1D). Cellular uptake experiments revealed a positive correlation between DPPS content and macrophage targeting efficacy, indicating the potential role of DPPS in enhancing cellular interactions (Fig. 1E and G). Cellular uptake

A

Library A: DoE array table (molar ratio)

	DSPC	DPPS	Chol	Man-PEG-DSPE
A1	0	100	0	0
A2	0	90	0	10
A3	0	50	50	0
A4	0	40	50	10
A5	100	0	0	0
A6	90	0	0	10
A7	50	0	50	0
A8	40	0	50	10
A9	35	35	25	5
A10	17.5	67.5	12.5	2.5
A11	17.5	62.5	12.5	7.5
A12	17.5	42.5	37.5	2.5
A13	17.5	37.5	37.5	7.5
A14	67.5	17.5	12.5	2.5
A15	62.5	17.5	12.5	7.5
A16	42.5	17.5	37.5	2.5
A17	37.5	17.5	37.5	7.5

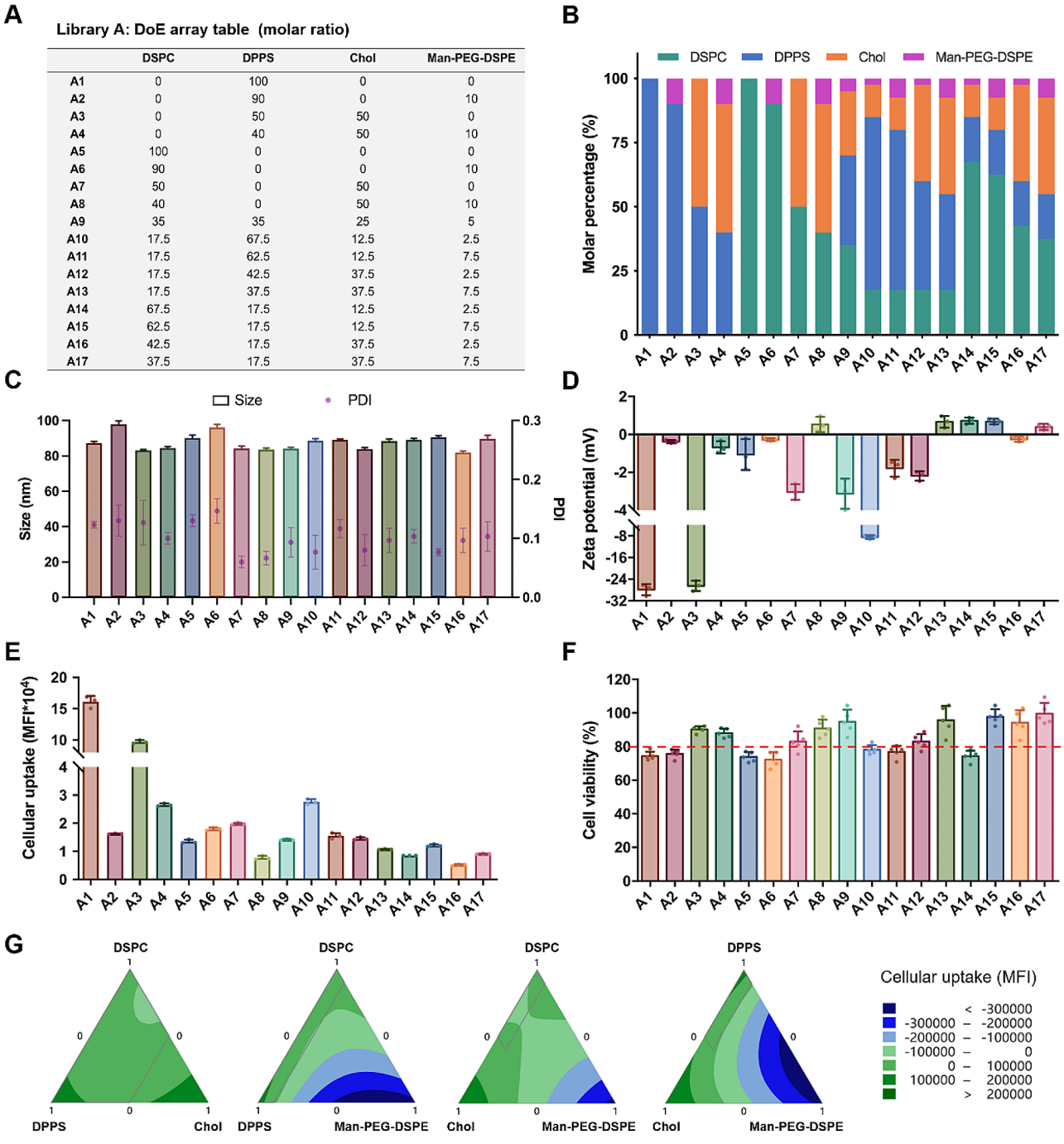

Fig. 1 DoE strategy for optimizing liposome composition ratio in Library A. (**A**) Details of liposomal formulations in Library A for first-round optimization of macrophage-targeting liposomes, including the determinate molar ratios of each component in liposomes. (**B**) Molar ratios of the designed liposomes in Library A. (**C**) Particle sizes, PDI and (**D**) Zeta potentials of the prepared liposomes in Library A ($n = 3$). (**E**) Flow cytometry analysis of cellular uptake and (**F**) Cell viability of different liposomal formulations in Library A on RAW 264.7 cells ($n = 3$). (**G**) Response contour plot for DPPS, DSPC, Chol, and Man-PEG-DSPE (respectively). The colored contour bands show ranges of different mean fluorescence intensity (MFI) values obtained from flow cytometry experiments ($n = 3$)

decreased as the PEG content increased, reminding that a balanced PEG concentration to maintain targeting specificity and cellular internalization (Fig. 1E). Results from cell cytotoxicity assay showed that in most cases Chol content below 20% induced considerable toxicity, while formulations with DPPS exceeding 30%, and Chol combined with DSPC below 40%, also increased cytotoxicity. Meanwhile, DPPS content exceeding 60% was also associated with increased cytotoxicity (Fig. 1F). Based on the results above, further optimization guidelines were established, stipulating molar composition as that Chol content (20 −50%), DSPC≥20%, DPPS≤60% and the molar proportion of Man-PEG-DSPE was fixed to constitute 2% of the total lipid content, which included Chol, DSPC, and DPPS. As shown in Table S1, liposomes in Library B with 9 formulations were generated and prepared. These liposomes showed a more uniform particle size (80–90 nm) as Man-PEG-DSPE fixed at 2%, and PDI was below 0.2 as well (Figure S2A). As shown in Figures S2B and S2C, zeta potential decreased and cellular uptake increased as DPPS increased, consistent with that of Library A. No obvious cell toxicity was observed when co-cultured with RAW264.7 cells for 24 h (Figure S2D). The DoE mixed formulation analysis towards cellular uptake indicated that PS modification significantly influenced the cellular uptake of liposomes by macrophages (Figure S3). Among the nine liposomal groups, those with higher levels of DPPS exhibited a notable increase in targeted cellular uptake compared to their counterparts with lower DPPS content. This underscored the pivotal role of PS in enhancing the affinity of liposomes for macrophages, promoting efficient cellular internalization. Thus, in the absence of apparent cytotoxicity, augmenting the PS content in liposomes represented a viable strategy to enhance their macrophage-targeting capabilities.

Altogether, these results highlighted the intricate interplay of liposomes' components in influencing both targeting specificity and cytotoxicity. The use of PS modification in liposomes to mimic apoptotic signals for macrophage targeting holds significant promise for improving drug delivery precision. Results of the cellular uptake experiments have shown that the extent of PS modification in liposomes was directly correlated with the targeting efficiency towards macrophages. As the surface density of PS increases, the recognition and uptake of liposomes by macrophages also rose proportionally. This heightened targeting specificity holds promise for the precise delivery of therapeutic agents to sites associated with macrophage activation, such as inflamed tissues or tumor microenvironments. Conversely, the elevated PS modification raised concerns about the potential unwanted cytotoxic effects. The same high affinity for macrophages that enhances targeting may also result in unintended interactions with healthy cells, leading to increased toxicity. Therefore, it becomes crucial to strike a delicate balance in PS modification to achieve optimal targeting without compromising safety. As to PEG, it has been a common strategy that the incorporation of PEG into liposomes enhances their in vivo circulation time by reducing opsonization and clearance by the reticuloendothelial system. However, excessively high concentrations of PEG may compromise the efficacy of PS-modified liposomes in targeting macrophages, which was attributed to the reduced ability of PEGylated liposomes to interact with macrophages, thus hindering the specific recognition and uptake mediated by PS modification [27]. In addition, the introduction of Chol contributes to the creation of liposomes that closely mimic natural cell membranes [28]. By enhancing membrane stability, improving circulation, and modulating liposome-membrane interactions, Chol contributes to the development of biocompatible liposomal delivery systems. While Chol proves beneficial in enhancing liposome biocompatibility, the optimal Chol content in liposomal formulations requires careful consideration. Too little cholesterol may not provide the desired stabilizing effects, while excessive cholesterol can alter membrane fluidity and compromise therapeutic efficacy.

Therefore, through a thorough exploration of various lipid components via the DoE strategy, we have arrived at a refined molar ratio for the liposome formulation that optimally addresses the intricate balance between macrophage targeting and reducing cellular toxicity in liposomal formulations. The final chosen molar ratio, DSPC: DPPS: Chol: Man-PEG-DSPE=20:60:20:2, represented a harmonious blend that caters to both macrophage targeting specificity and cellular biocompatibility.

TaE approach fine-tuned the lipid composition of liposomes

Combined with the DoE strategy, the TaE approach was employed to fine-tune liposomal formulations based on empirical observations. Iterative adjustments were made to optimize the liposomal characteristics, ensuring the replication of apoptotic cell features critical for effective macrophage targeting. This pragmatic approach complemented the systematic DoE strategy, allowing for flexibility in addressing unforeseen challenges and enhancing the likelihood of successful formulation development.

The influence of phospholipid structural variations, specifically differences in fatty acid chain length and saturation, on the targeting efficiency and toxicity of PS-presenting liposomes in macrophage interactions was a critical aspect of our study. The length of fatty acid chains in phospholipids is known to impact membrane fluidity and lipid packing. Meanwhile, the degree of saturation in fatty acid chains also plays a pivotal role in shaping liposomal characteristics. In addition,

phosphatidylglycerol (PG), being a key constituent of Gram-negative bacterial cell membranes, possesses distinctive features that may influence its interactions with macrophages [29]. The negative charge associated with PG could potentially contribute to improved recognition and uptake by macrophages, mirroring the electrostatic interactions observed in bacterial-host cell interactions. This unique property of PG may open new possibilities for tailoring liposomal formulations to mimic the characteristics of Gram-negative bacteria for targeted drug delivery. Therefore, the impact of PS and PG structural modifications with varying fatty acid chain lengths and saturation levels on macrophage targeting and cytotoxicity was investigated through the TaE approach. Three distinct PS structures, namely DPPS, 1,2-dioleoyl-*sn*-glycero-3-phospho-L-serine (DOPS), and 1,2-distearoyl-*sn*-glycero-3-phospho-L-serine (DSPS), were selected for examination, alongside three PG structures—1,2-dipalmitoyl-*sn*-glycero-3-phosphoglycerol (DPPG), 1,2-dioleoyl-*sn*-glycero-3-phosphoglycerol (DOPG), and 1,2-distearoyl-*sn*-glycero-3-phosphoglycerol (DSPG)—chosen based on their comparable fatty acid chain lengths and saturation degrees (Figure S4).

Six kinds of liposomes with fixed ratios were prepared by TaE approach (Table S2). The average size was 90 nm with PDI < 0.2 (Fig. 2A). Negative potential extended with longer fatty acid chain length and higher saturation(Fig. 2B). In the context of cellular uptake experiments, the results revealed that liposomes modified with DSPS and DOPG exhibited the highest efficiency in macrophage uptake (Fig. 2C), suggesting that the specific structural features of DSPS and DOPG contribute to enhanced recognition and internalization by macrophages, pointing towards their potential as promising candidates for targeted drug delivery systems. However, it is crucial to note that, despite their high targeting efficiency, liposomes modified with DOPG demonstrated a higher level of cytotoxicity (Fig. 2D). This observation underscored the importance of carefully considering not only the targeting efficacy but also the safety profile of the modified liposomes. Balancing these factors is essential to developing effective therapeutic strategies that minimize potential adverse effects. Therefore, DSPS was chosen to replace DPPS for further study. In addition, we also evaluated three PC-structure three phospholipids with different fatty acid chain lengths and saturation of phospholipids (Figure S5). As shown in Table S3 and Fig. 2E and H, three kinds of liposomes have been made with an average size of 90 nm, PDI < 0.2 and negative potential corresponded to Fig. 2B. 1,2-Dioleoyl-*sn*-glycero-3-phosphocholine (DOPC) showed the highest cell uptake and no obvious cytotoxicity. Thus, DOPC was chosen to replace DSPC.

Further, we designed a series of liposomes to verify the effects of PS structure, PEG content, and Man modification on macrophage targets (Table S4). As shown in Fig. 3A and B, uniform liposomes have been prepared with an average size of 90 nm, PDI < 0.2. The lower zeta potential corresponds to increased DSPS ratio in liposomes and approached neutralization with higher PEG. In the group of 2% PEG, Man modification showed no effects on cellular uptake, whereas cell uptake increased with Man modification. Cellular uptake significantly increased in the PS group than in the PC group, however,

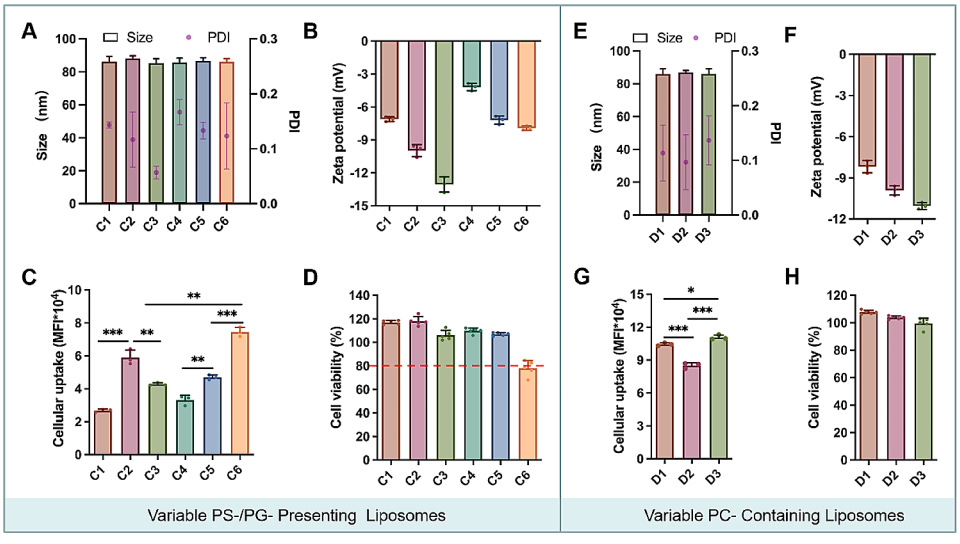

Fig. 2 TaE approach for fine-tuning the lipid composition of liposomes. (**A**) Particle sizes, PDI and (**B**) Zeta potentials of the prepared liposomes in Library C ($n = 3$). (**C**) Flow cytometry analysis of cellular uptake and (**D**) Cell viability of different liposomal formulations in Library C on RAW 264.7 cells ($n = 3$). (**E**) Particle sizes, PDI and (**F**) Zeta potentials of the prepared liposomes in Library D ($n = 3$). (**G**) Flow cytometry analysis of cellular uptake and (**H**) Cell viability of different liposomal formulations in Library D on RAW 264.7 cells ($n = 3$). Data were expressed as the mean ± SD, *$p < 0.05$; **$p < 0.01$; ***$p < 0.001$

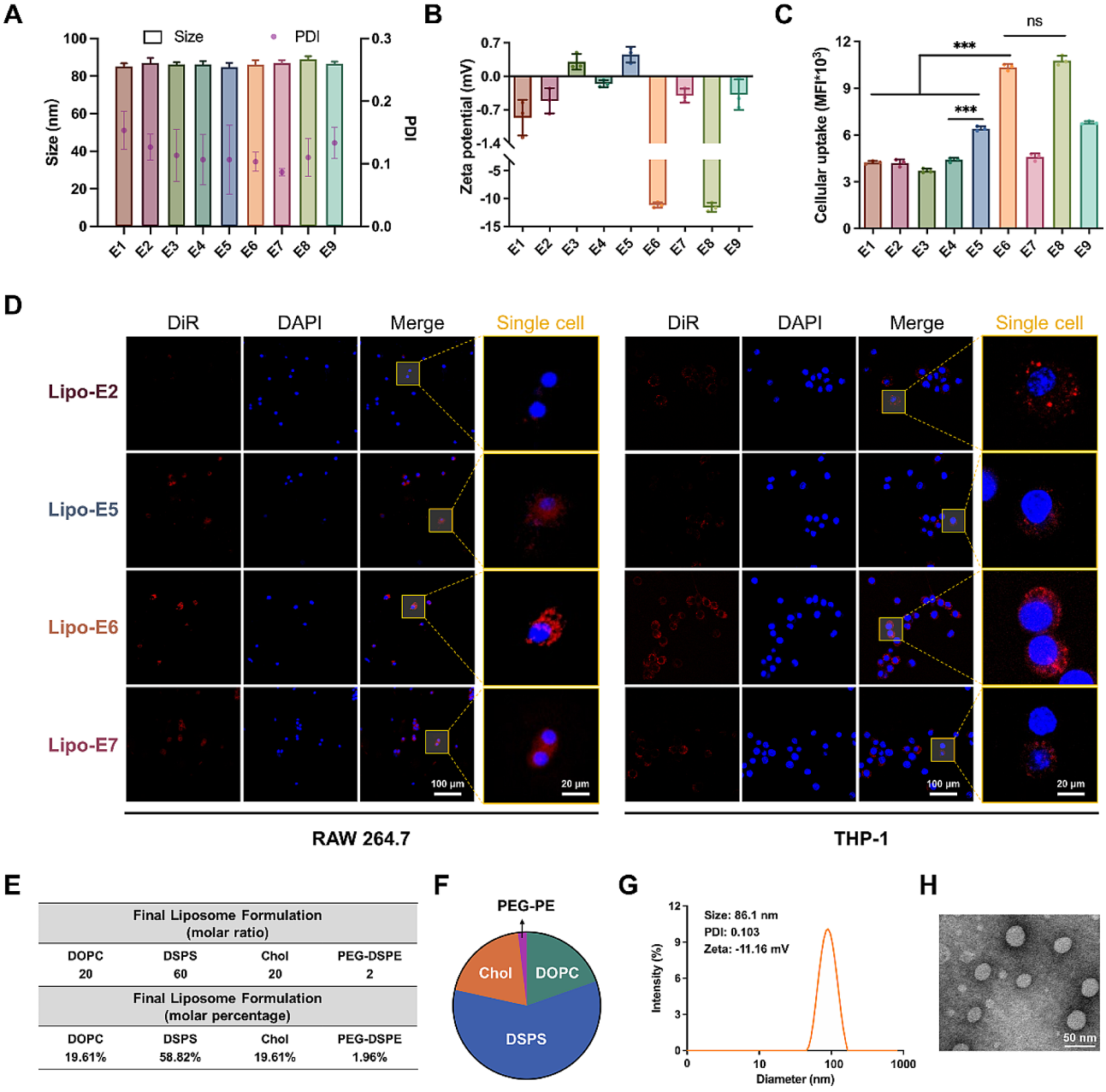

Fig. 3 (**A**) Particle sizes, PDI and (**B**) Zeta potentials of the prepared liposomes in Library E ($n=3$). (**C**) Flow cytometry analysis of cellular uptake of different liposomal formulations in Library E on RAW 264.7 cells ($n=3$). (**D**) Confocal microscopic images of cellular internalization of different DiD-loaded liposomes after 1 h incubation with RAW 264.7 and THP-1 cells. Cell nuclei were stained by Hoechst (blue). The scale bar is 100 μm and 20 μm. (**E**) The determinate liposomal formulation after DoE and TaE screening. (**F**) The molar percentage of the optimized liposomal formulation. (**G**) Characterization summary of the optimized liposomes with a molar ratio of 20:60:20:2 (DOPC/DSPS/Chol/PEG-DSPE) (**H**) TEM image of the optimized liposomes stained by phosphotungstic acid solution (scale bar: 50 nm). Data were expressed as the mean ± SD, ***$p < 0.001$; ns, not significant

the PEG up to 60% offset the PS effect (Fig. 3C). The most significant cellular uptake of Lipo-E6 by RAW 264.7 and THP-1 was observed by confocal laser scanning microscopy (CLSM) (Fig. 3D). Accumulated data inspired us that PS modification improves macrophage target, while Man modification did not show obvious effects on macrophage target, which could be due to the discrepancy in CD206 expression (Figure S6). Thus, PEG-PE composition of liposomes would be used for further study (final formulation DOPC: DSPS: Chol: PEG-PE=20:60:20:2, molar ratio), and the average size was 86.1 nm and zeta potential was −11.16 mV (Fig. 3E-H). Interestingly, the above results showed that as the PS modification increased, the zeta potential decreased, while the cellular uptake of the liposomes increased. The PS modification, despite reducing the positive charge of

the liposomes, enhanced their specificity and uptake by macrophages due to the strong targeting affinity of PS for these cells. This targeted interaction is crucial for applications where precise delivery to macrophages is desired.

The observed differences in targeting efficiency among different phospholipids suggested that the structural variations in fatty acid chains contribute to the modulation of macrophage interactions. However, it is crucial to acknowledge that while certain modifications enhance targeting efficiency, they may concurrently increase cytotoxicity. Achieving an optimal balance between efficient macrophage targeting and minimal cytotoxic effects is essential for the development of safe and effective PS-modified liposomal drug delivery systems. The findings underscored the complexity of the relationship between phospholipid structure, PS/PG modification, and cellular responses. Further research and optimization efforts should aim to elucidate the underlying mechanisms governing these effects. Strategies to fine-tune the fatty acid chain characteristics, such as exploring different ratios of saturated to unsaturated lipids, may provide avenues for tailoring liposomal formulations to achieve the desired balance of targeting efficiency and reduced toxicity.

Evaluation of the potential of identified liposomes to target macrophage in murine inflammatory models

The transition from in vitro screening to in vivo validation represents a critical phase in the development of liposomal formulations for targeted therapy. Thus, following the in vitro screening process to identify the optimal liposomal formulation, three well-established murine inflammatory models, including colitis, rheumatoid arthritis (RA), and lung inflammation (Figure S7), were used to validate the targeting specificity of the optimized liposomal formulation at inflammation sites through the in vivo biodistribution imaging. As a control, liposomes composed of DSPC, Chol, and PEG-PE were used, named PC-presenting liposomes (PC-Lipo). PC-Lipo and PS-presenting liposomes (PS-Lipo) were labeled with DiR for *in/ex vivo* imaging.

Firstly, the in vivo distribution of PC-Lipo and PS-Lipo was investigated in healthy BALB/c mice following intravenous tail vein injection of free DiR dye, and PC-Lipo/DiR and PS-Lipo/DiR. After 24 h, the mice were euthanized, and major organs were dissected for fluorescence imaging. As shown in Figures S8 and S9, fluorescence signals of PC-Lipo/DiR group were highest in all organs, excluding the lungs. Interestingly, in the lungs, both PC-Lipo/DiR and PS-Lipo/DiR groups exhibited relatively lower fluorescence signals. The difficulty in achieving substantial lung distribution may be attributed to the intricate pulmonary microenvironment. The pulmonary environment presents unique challenges for liposomes accumulation, and the rapid blood flow and low vascular permeability in the lungs likely contribute to the reduced accumulation observed. Additionally, the observed fluorescence in other tissues indicated a potential preference for non-pulmonary organs, which may influence the overall biodistribution of these liposomal formulations. Besides, most accumulation of PC-Lipo/DiR and PS-Lipo/DiR was observed in the liver and spleen where macrophages populate [30].

Then, three murine inflammatory models were established and used to study the in vivo biodistribution of free DiR dye, PC-Lipo/DiR, and PS-Lipo/DiR. These models were selected due to the enrichment of macrophages at the sites of inflammation. In the DSS-induced colitis model (Fig. 4A), a remarkable accumulation of liposomes was observed in the intestines compared to the control group (Fig. 4C and D). Hematoxylin and eosin (H&E) staining images showed inflammation and necrosis in intestines, indicating the successful colitis model (Fig. 4B). Besides, as shown in Figure S10A and D, both immunohistochemistry (IHC) and flow cytometry experiments indicated a significant increase in macrophage infiltration in inflamed intestines. These results supported the potential of the liposomes could be recruited to the inflamed regions by macrophages. We further varied macrophage-targeting in the collagen II-induced RA model (Fig. 4E). H&E images indicated the synovium inflammation and Safranin O/Fast green staining showed the cartilage degeneration (Fig. 4F), altogether to verify the success of the RA model. Increased macrophage levels were also observed (Figure S10B and E). PS-Lipo/DiR exhibited higher fluorescence signals in the mouse paws compared to PC-Lipo/DiR (Fig. 4G and H). In addition, as shown in Figures S11 and S12, while PS-Lipo/DiR showed a higher accumulation at the sites of inflammation, its distribution in other major organs remained similar to that observed in healthy mice. These results demonstrated excellent inflammation-targeting specificity of PS-Lipo. This observation aligns with the known affinity of PS for macrophages, confirming the potential of PS modification to enhance the targeted delivery of liposomes to inflammatory sites. In a recent study, Deprez J et al. showed that the selective depletion of circulating myeloid cells reduced the accumulation of liposomes by up to 50–60%, which suggested that myeloid-cell-mediated transport accounted for more than half of the liposomal accumulation in inflamed regions [31]. This study implied that PS-presenting liposomes were likely to bind to a large number of immune cells in the bloodstream, including macrophage precursor monocytes. Theoretically, any immune cell capable of recognizing and phagocytosing PS signals has the potential to bind to PS-presenting liposomes. During inflammatory responses, an increased number of immune cells, including macrophages and their precursors, are

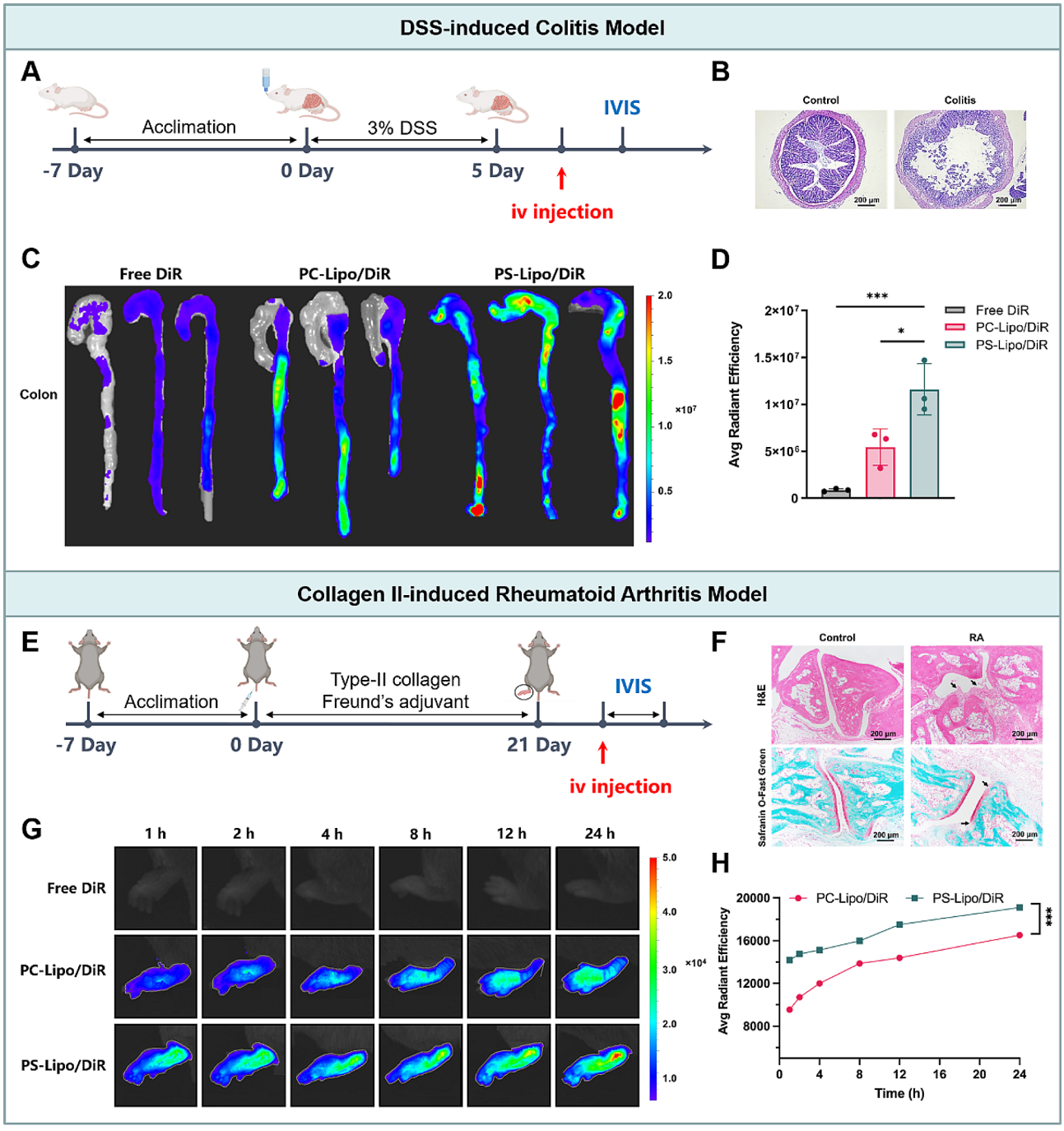

Fig. 4 In vivo murine inflammatory models assessing targeting of PS-presenting liposomes to macrophages. (**A**) Timeline of the DSS-induced colitis model study, showing a 7-day acclimation period for the mice, followed by a 5-day exposure to 3% DSS, culminating in in vivo imaging system (IVIS) monitoring post intravenous injection. (**B**) Histological comparison of colon sections from control mice and those with DSS-induced colitis, stained with H&E. The scale bar is 200 μm. (**C**) IVIS images of mice colons showing the distribution of free DiR and DiR-loaded liposomes (PC-Lipo/DiR and PS-Lipo/DiR). (**D**) Quantitative analysis of the fluorescent signal intensity from the DiR dye. (**E**) Timeline of the collagen II-induced RA model study, outlining the procedure from acclimation to arthritis induction with type-II collagen and Freund's adjuvant, and followed by IVIS monitoring after intravenous injection. (**F**) Histological examination of joint sections comparing healthy control mice to those with induced RA, using both H&E staining and Safranin O-fast green staining to highlight differences in tissue structure. The scale bar is 200 μm. (**G**) Temporal IVIS imaging sequence over 24 h showing the accumulation of free DiR and DiR-loaded liposomes (PC-Lipo/DiR and PS-Lipo/DiR) in the paws of mice. (**H**) Graphical representation of the quantified fluorescent signals over time, indicating the increased uptake of PS-Lipo/DiR in the inflamed paws of mice. Data were expressed as the mean ± SD, *$p < 0.05$; ***$p < 0.001$

recruited to the inflammatory sites. PS-presenting liposomes were designed to target macrophages or other PS-recognizing immune cells, enabling passive targeting of the inflammatory regions due to the increased presence of immune cells, which ensured that the liposomes were efficiently directed to the sites where they were needed most.

However, in the lipopolysaccharide (LPS)-induced lung inflammation model, a notable discrepancy was observed, and both PC-Lipo and PS-Lipo failed to reach the pulmonary tissues (Figure S13), which was consisted with the observation in healthy mice. The comparable or even lower fluorescence levels between the two groups in the lungs suggested that PS modification did not exacerbate or alleviate the challenge of lung delivery compared to PC-Lipo. The inability of PS-Lipo to reach the lungs may be attributed to the distinct pathophysiological environments of different tissues or the more widely accepted view that the formation of a protein corona affected their in vivo distribution. The formation of the protein corona significantly alters the surface characteristics of nanoparticles, thus greatly affecting their interactions with organs and cells. In a recent study, Le ND et al. synthesized a series of poly(β-amino ester) (PBAE) derivatives and found that the protein corona on nanoparticles could help achieve organ targeting (lungs and spleen) [32]. Interestingly, their findings correlated closely with the study of Min Qiu et al. [33] , which demonstrated that the protein corona on lung-targeted nanoparticles had distinct characteristics that promoted lung accumulation. The protein corona formed on the surface of liposomes is primarily influenced by the physicochemical properties of the liposomes themselves. By selecting different lipid components or varying their ratios, it is possible to achieve targeting of different organs or cells. In 2020, Daniel Siegwart et al. reported a Selective Organ Targeting (SORT) delivery technology [34]. They introduced the cationic lipid DOTAP as a fifth component to the formulation 5A2-SC8/DOPE/DMG-PEG2000/Cholesterol, thereby altering the physicochemical properties of the LNPs, including their zeta potential. This modification influenced the formation of the protein corona during blood circulation, enabling intravenous delivery of mRNA to the lungs. Recently, Daniel Siegwart's team reporting the use of Lung SORT LNPs for delivering ABE mRNA/sgRNA to perform gene editing on lung stem cells, treating pulmonary cystic fibrosis [35]. These findings highlight the complexity and potential of manipulating nanoparticle properties and their protein corona to achieve targeted delivery to specific organs, including the lungs. Therefore, one promising avenue involves the introduction of cationic lipids into the liposomal formulation, which may introduce a more balanced surface charge to achieve lung-targeting. However, the exact mechanisms and optimal strategies require further investigation to enhance the efficacy of lung-targeted liposomal delivery systems.

In addition, pharmacokinetic experiment was conducted to investigate the pharmacokinetic profiles of PC-Lipo and PS-Lipo in mice. As shown in Fig. 5C, PS-Lipo exhibited a faster metabolic rate compared to PC-Lipo. Specifically, 50% of PS-Lipo was metabolized within the first 2 h post-injection, and nearly 80% was cleared from the body within 24 h. This rapid clearance of PS-Lipo can be attributed to the enhanced recognition and removal by the body's clearance mechanisms, likely due to the PS modification that mimicked apoptotic signals. This facilitated the recognition and phagocytosis by immune cells, leading to quicker elimination from the body. Consequently, this rapid metabolism of PS-Lipo not only underscored its efficient clearance but also implied a potentially lower systemic exposure and toxicity, enhancing its safety profile for in vivo applications. In contrast, PC-Lipo demonstrated a slower metabolic rate, resulting in prolonged circulation time within the body. This extended presence in the bloodstream likely contributed to the notable accumulation of PC-Lipo in the liver and spleen, leading to a higher degree of uptake and accumulation in these organs compared to PS-Lipo.

Therefore, the distinct behavior of PS-Lipo in different inflammatory models underscored the context-dependent nature of their targeting efficacy. While PS modification enhanced macrophage targeting in certain inflammatory conditions, its effectiveness appeared to be compromised in the pulmonary environment. This highlighted the importance of considering the specific characteristics of each target tissue and disease context when designing targeted drug delivery systems, and potential strategies such as the introduction of cationic lipids may be explored to overcome this limitation and improve their overall efficacy in diverse inflammatory settings.

Biocompatibility evaluation in vivo

Understanding the interaction between liposomes and biological systems is essential to ensure their safety and efficacy for clinical transformation applications. Therefore, the in vivo biocompatibility of PC-Lipo and PS-Lipo has been evaluated in BALB/c mice. Mice were injected with saline, PC-Lipo, or PS-Lipo every two days, and their body weights were recorded. After two weeks, the mice were euthanized, and major tissues and blood were collected for analysis. Tissues were stained with H&E to assess for tissue damage and inflammatory reactions. As shown in Fig. 5A, no significant histological changes such as necrosis or inflammation have been observed in organs as heart, liver, spleen, lung, and kidney. Hematological parameters, encompassing red blood cell (RBC) count, white blood cell (WBC) count, hemoglobin level

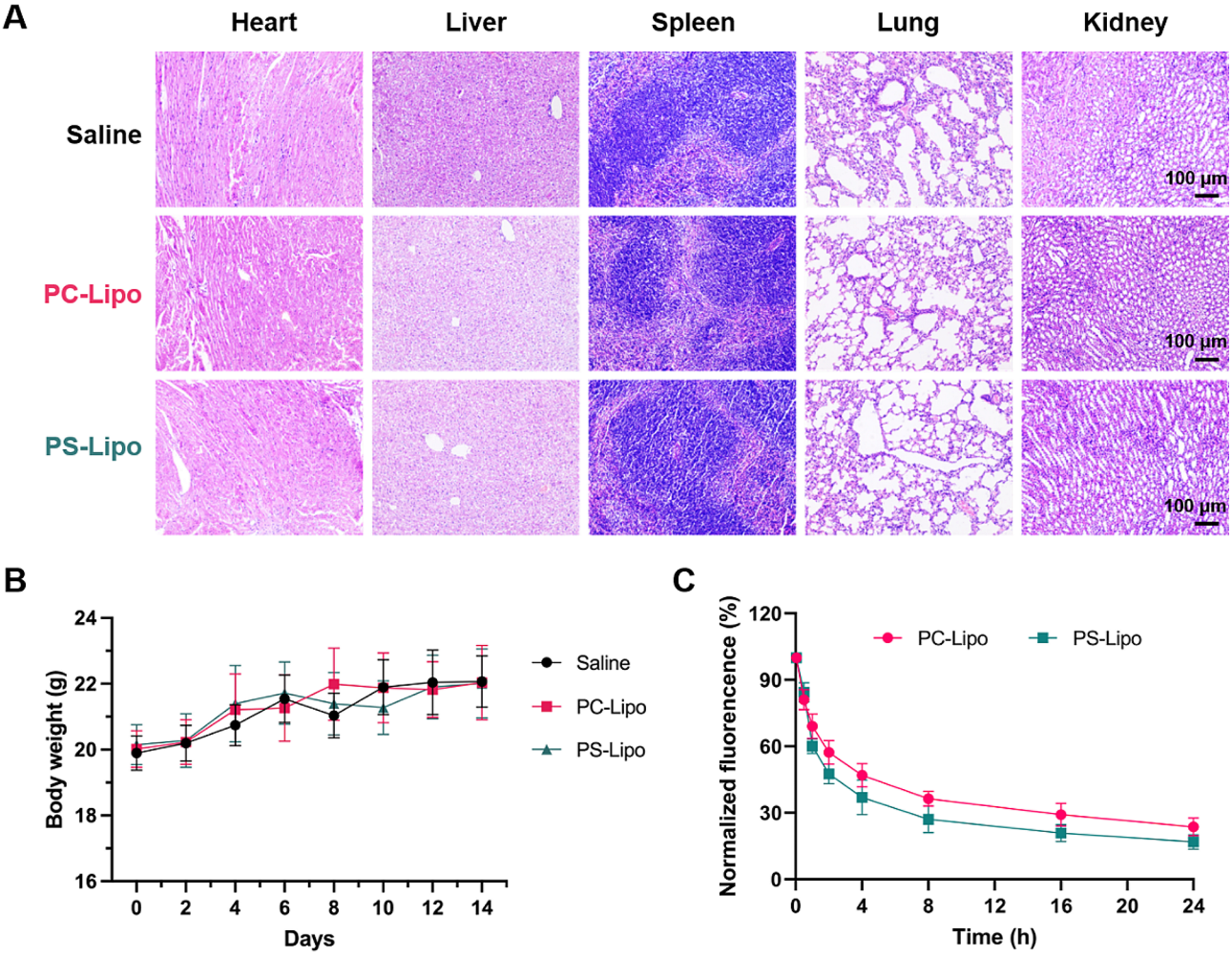

Fig. 5 Evaluation of in vivo biocompatibility and pharmacokinetics of liposomes in healthy BALB/c mice. (**A**) Histopathological analysis of heart, liver, spleen, lung, and kidney tissues stained with H&E. Tissues were collected from subjects treated with saline (control), PC-Lipo, and PS-Lipo. The scale bar is 100 μm. (**B**) Body weight changes over a 14-day period following treatment with saline (control), PC-Lipo, and PS-Lipo ($n = 3$). (**C**) Pharmacokinetic profiles of DiD-labeled PC-Lipo and PS-Lipo in mice following once administration ($n = 3$). Data were expressed as the mean ± SD

(HBL), as well as biomarkers including aminotransferase (ALT), aspartate aminotransferase (AST), and creatinine (CREA), collectively indicated the biocompatibility and safety of the liposomes for major organs, with no discernible toxicity observed in the hematologic system, liver, or kidney (Figure S14). The body weight was also monitored and showed a steady increase for 2 weeks (Fig. 5B), indicating that the liposomes did not induce substantial stress or alterations in the metabolic status of the animals.

These encouraging findings showed the potential application of the liposomal formulation in various therapeutic contexts with excellent biocompatibility. However, it is essential to note that this study is a preliminary assessment, and further investigations, including long-term studies and drug or bioactive molecules delivery, may contribute to providing a more comprehensive understanding of the liposomes.

Therefore, based on the current study, the prepared liposomes exhibit promising in vivo biocompatibility in female BALB/c mice. These results lay the foundation for future research and development, emphasizing the importance of continued safety assessments to ensure the translational potential of the liposomal formulation in clinical and biomedical applications.

Conclusion

In conclusion, this study employed a combination of DoE strategy and TaE approach to screen the optimal formulation of PS-presenting liposomes, aiming to target macrophages effectively while ensuring low cytotoxicity. In vivo validation was conducted in three mouse inflammation models to confirm the macrophage-targeting capability of the liposomes. While the liposomes demonstrated excellent macrophage targeting in colitis and RA models, their targeting ability in lung inflammation

model was hindered, indicating the need for further optimization to target lung inflammation. The assessment of liposomal biocompatibility in vivo yielded promising results, suggesting a potential for clinical translation. Overall, this study highlighted the importance of optimizing liposomal formulations for specific inflammatory conditions and underscored the potential clinical utility of PS-presenting liposomes as targeted drug delivery systems. The identified optimal range for each component provided valuable insights for the rational design of liposomes tailored for macrophage targeting, holding promise for future applications in drug delivery and therapeutic interventions.

Experimental section

Materials

1,2-dipalmitoyl-*sn*-glycero-3-phosphocholine (DPPC), 1,2-dipalmitoyl-*sn*-glycero-3-phospho-(1'-rac-glycerol) (sodium salt) (DPPG) and 1,2-distearoyl-sn-glycero-3-phosphoethanolamine-N-[carboxy(polyethylene glycol)-2000, NHS ester] (sodium salt) (DSPE-PEG_{2000}-NHS) were purchased from Avanti Polar Lipids, Inc. (Alabaster, USA). 1,2-dipalmitoyl-*sn*-glycero-3-phospho-L-serine (sodium salt) (DPPS) was purchased from Corden Pharma Switzerland LLC (Liestal, Switzerland). 1,2-dioleoyl-*sn*-glycero-3-phosphocholine (DOPC), 1,2-distearoyl-*sn*-glycero-3-phosphocholine (DSPC), 1,2-dioleoyl-*sn*-glycero-3-phospho-(1'-rac-glycerol) (sodium salt) (DOPG), cholesterol (Chol) and 1,1'-dioctadecyl-3,3,3',3'-tetramethylindodicarbocyanine perchlorate (DiD) were purchased from Macklin Biochemical Technology Co., Ltd (Shanghai, China). 1,2-distearoyl-*sn*-glycero-3-phospho-(1'-rac-glycerol) (sodium salt) (DSPG) and 1,2-distearoyl-sn-glycero-3-phosphoethanolamine-N-[methoxy(polyethylene glycol)-2000] (ammonium salt) (DSPE-PEG_{2000}) were purchased from Xi'an Ruixi Biological Technology Co., Ltd (Xi'an, China). 1,2-dioleoyl-*sn*-glycero-3-phospho-L-serine (sodium salt) (DOPS) was purchased from Yuanye Bio-Technology Co., Ltd (Shanghai, China). 1,2-distearoyl-*sn*-glycero-3-phospho-L-serine (sodium salt) (DSPS) was purchased from Highfine Biotech Co., Ltd (Suzhou, China). 3,3'-dioctadecyloxacarbocyanine perchlorate (DiO) was purchased from Aladdin Biochemical Technology Co., Ltd. (Shanghai, China). Triethylamine (TEA) was purchased from Sinopharm Chemical Reagent Co., Ltd (Shanghai, China). Lipopolysaccharide (LPS), phorbol 12-myristate 13-acetate (PMA), Type II collagen, and incomplete Freund's adjuvant (IFA) were purchased from Sigma-Aldrich (Saint Louis, USA). Cell counting kit-8 (CCK-8), 4',6-diamidino-2-phenylindole dihydrochloride (DAPI), and phosphate-buffered saline (PBS) were purchased from Beyotime Biotech. Inc. (Shanghai, China). Dulbecco's Modified Eagle Medium (DMEM) and fetal bovine serum (FBS) were purchased from Gibco (Thermo Fisher Scientific, China). Dextran sulfate sodium (DSS) with a molecular weight of 36 to 50 kD was purchased from MP Biomedicals (Solon, USA). All organic solvents were purchased from Merck (Darmstadt, Germany).

Design of experiment (DoE)

The Design of Experiment (DoE), as a versatile statistical tool, enables a structured exploration of the multifaceted parameter space involved in liposomal development and has emerged as a powerful and systematic approach for optimizing the formulation of liposomes. Mixture design was selected to identify the optimal conditions that contribute to maximizing macrophage targeting and minimizing cytotoxicity, which could strategically evaluate and manipulate critical formulation variables, such as lipid composition, size, and surface modifications, to discern their individual and collective impacts on liposomal characteristics. The screening study was performed to identify the main relevant parameters determining the macrophage targeting of liposomes to RAW 264.7 cells. Experiments were designed and data were analyzed using Minitab Version 17.0 software (Minitab Inc., State College, USA).

Preparation and characterization of liposomes

DSPE-PEG_{2000}-Mannose (DSPE-PEG_{2000}-Man) was synthesized by covalent conjugation of DSPE-PEG_{2000}-NHS and 4-aminophenyl α-D-mannopyranoside with a simple one-step reaction. The product DSPE-PEG_{2000}-Man was purified by dialysis with a molecular weight cut-off of 3500 Da and confirmed by ^{1}H nuclear magnetic resonance (NMR) using Varian 400 MHz (Bruker, Germany), and chemical shifts were expressed as parts per million (ppm).

The liposomes were prepared by the thin-film hydration method according to previous works [36, 37]. Briefly, lipids with varying proportions and compositions were dissolved in chloroform/methanol (90/10, v/v). Then, the organic solvent was removed by rotary evaporation, and the film was hydrated in PBS by mild sonication. Finally, the lipid dispersion was extruded 31 times through polycarbonate filters (pore size 200 nm) using a mini-extruder (Avanti, USA) to obtain desired liposomes. DiO- or DiD-loaded liposomes were prepared by adding DiO or DiD to the organic solution of lipids before solvent evaporation.

Particle size distribution and zeta potential of prepared liposomes were measured by were measured by dynamic light scattering (DLS) on a Delsa™ Nano C Particle Analyzer (BECKMAN COULTER, USA) at 25 °C. The morphology of liposomes was examined by transmission electron microscopy (TEM) (JEOL JEM1010, Japan) with 2% (w/v) phosphotungstic acid staining. Briefly, 10 μL water-diluted suspension of the liposomes (about

0.05 mg/mL) was dropped on a 200-mesh carbon-coated copper grid which was left to dry. Then, 10 μL 2% (w/v) phosphotungstic acid was added and left in contact with the sample for 5 min.

Cell culture

The mouse monocyte macrophage cell line RAW 264.7 was obtained from the Cell Bank of the Chinese Academy of Sciences (Shanghai, China) and grown in DMEM medium supplemented with 100 U/mL penicillin, 100 μg/mL streptomycin, and 10% FBS at 37 °C in a humidified 5% CO_2/95% air atmosphere. THP-1 monocyte cell line was kindly provided by Prof. Shengnan Li from the Department of Pharmacology, Nanjing Medical University, China. The differentiation of THP-1 monocytes into macrophages involves a straightforward protocol. Initially, THP-1 monocytes are cultured in RPMI-1640 medium supplemented with 100 U/mL penicillin, 100 μg/mL streptomycin, and 10% FBS at 37 °C in a humidified 5% CO_2/95% air atmosphere. The induction of macrophage differentiation is achieved by treating the monocytes with 100 ng/mL PMA for 24 to 48 h. Following this induction, the PMA is removed, and the cells are allowed to mature in a fresh medium without PMA for an additional 24 to 48 h. During this period, macrophage adherence and morphology changes are observed. Successful differentiation is confirmed by the characteristic spread-out and adherent appearance of macrophages. The resulting macrophages can then be harvested for downstream experiments or analysis.

Cellular uptake of liposomes by flow cytometry

The cellular uptake of liposomes was determined in RAW 264.7 cells by flow cytometry. Briefly, the cells were seeded into 12-well plates at a density of 1.5×10^5 cells/well and incubated overnight, followed by the incubation with DiO- or DiD- labeled liposome formulations (DiO or DiD, 2 μM) in the cell culture medium for 1 h. Then, the cells were harvested by gentle pipetting and centrifugation at 1000 rpm for 5 min, resuspended in 400 μL of PBS, and analyzed by a flow cytometer (CytoFLEX, Beckman Coulter, USA). The untreated cells served as the negative control.

Intracellular distribution of liposomes by confocal microscopy

To observe the intracellular distribution and the fluorescence intensity of liposome formulations, we used confocal microscopy. For this purpose, RAW 264.7 cells and THP-1 monocytes-derived macrophages were seeded into 6-well plates at a density of 1×10^5 cells/well and incubated with DiD-labeled liposome formulations (DiD, 2 μM) for 1 h. Cells were washed with PBS and fixed in 4% paraformaldehyde for 10 min, followed by stain with DAPI for 15 min. After washing with PBS three times, the cells were analyzed using a confocal laser scanning microscope (Carl Zeiss LSM 710).

Measurement of cell cytotoxicity in vitro by CCK8

The cytotoxicity of different liposome formulations on RAW 264.7 cells was investigated by using CCK-8 assay. In brief, RAW 264.7 cells were seeded into 96-well plates at 8×10^3 cells/well and incubated at 37 °C overnight before the treatment. Then, the medium was replaced with fresh medium containing different liposome formulations at the concentration of 500 μM total lipid for 24 h. Thereafter, cell viability was determined using a CCK-8 kit according to the manufacturer's instructions. Untreated cells were taken as control with 100% viability.

Analysis of CD206 expression on macrophages

RAW 264.7 cells were cultured and divided into three groups: untreated, M1-polarized, and M2-polarized. M1 polarization was induced by treating RAW 264.7 cells with lipopolysaccharide (LPS) at 100 ng/mL for 24 h. M2 polarization was achieved by treating RAW 264.7 cells with interleukin-4 (IL-4) at 20 ng/mL for 24 h. To assess CD206 expression, flow cytometry and western blotting were performed. For flow cytometry, cells from each group were stained with FITC-conjugated anti-CD206 antibody and analyzed using a flow cytometer to measure fluorescence intensity. For Western blotting, cells were lysed, and proteins were separated by SDS-PAGE, transferred to PVDF membranes, and probed with anti-CD206 antibody. Protein bands were visualized using enhanced chemiluminescence.

Animal experiments

Three kinds of mice, namely female BALB/c, male C57BL/6, and male DBA/1 mice, were provided by the Animal Center of Nanjing Medical University and fed at the condition of 25 °C and 55% humidity. All animal experiments were approved by the Animal Care and Use Committee of Nanjing University (IACUC-2003054) and under international regulations and standards on animal welfare. Mice were randomly divided in a blinded fashion at the beginning of each experiment.

DSS-induced colitis model

Mouse colitis was induced in 8-week-old female BALB/c mice using dextran sulfate sodium (DSS) according to a previous publication [38]. All mice were acclimatized for 1 week after arrival and randomly into three groups. Thereafter, mice were fed with 3% (wt/vol) DSS in drinking water for 7 days to establish the acute colitis model.

LPS-induced lung inflammation model

Mouse lung inflammation was induced in 8-week-old male C57BL/6 mice by intranasal instillation of LPS according to a previous publication [39]. All mice were acclimatized for 1 week after arrival and randomly into three groups. Under anesthesia by intraperitoneal injection of chloral hydrate (300 mg/kg), mice were positioned on the foam board for intranasal delivery of 20 μL LPS (5%, wt/vol) once daily for three days.

Collagen II-induced rheumatoid arthritis model

Mouse rheumatoid arthritis was induced in 8-week-old male DBA/1 mice by administering emulsified collagen II in incomplete Freund's adjuvant (IFA) [40]. All mice were acclimatized for 1 week after arrival and randomly into three groups. Then, mice were administered 50 μL of 5 mg/mL collagen II emulsion via the tail and challenged with 50 μL of 5 mg/mL collagen II emulsion three weeks later in a similar way. The immune system recognizes collagen II as foreign, initiating an autoimmune response that leads to inflammation in the joints, similar to the pathogenesis of rheumatoid arthritis in humans.

Validation of model establishment and macrophage enrichment

In order to validate the successful establishment of the three inflammation models—colitis, lung inflammation, and rheumatoid arthritis—we employed a combination of histological and immunological techniques. Mice were euthanized and dissected to obtain colon, lung, and joint tissues. Hematoxylin and Eosin (H&E) staining was performed on tissues collected from the colon, lung, and joints of model mice. Safranin-O/Fast Green was used to stain cartilage tissues. To further confirm the presence and extent of inflammation, immunohistochemistry (IHC) was performed using an antibody against F4/80, a specific marker for macrophages. Tissue sections from the colon, lung, and joints were stained and examined under a microscope to detect the presence of F4/80-positive macrophages. The intensity and distribution of F4/80 staining were evaluated to quantify macrophage infiltration in the respective tissues. Moreover, flow cytometry analysis was conducted to quantify the expression of macrophages in the inflamed tissues. Single-cell suspensions were prepared from the colon, lung, and joint tissues of the model mice. Cells were stained with FITC-conjugated antibody against F4/80. Flow cytometry was used to measure the proportion of F4/80-positive cells, providing a quantitative assessment of macrophage enrichment at the inflammation sites.

In vivo biodistribution and pharmacokinetic study

The in vivo animal imaging system was used to study the biodistribution of the prepared liposomes. To track the drug biodistribution, the NIR probe DiR was loaded onto the liposomes. For collagen II-induced rheumatoid arthritis model, the fluorescence of the mouse paw at 1 h, 2 h, 4 h, 8 h, 12 h, and 24 h upon injection was recorded using an IVIS spectrum imaging system. As to DSS-induced colitis model, the mice were sacrificed 24 h post the injection, and the intestines were collected and excised to analyze the ex vivo fluorescence. For LPS-induced lung inflammation model, the mice were sacrificed 6 h post the injection, and the major tissues, including heart, liver, spleen, lung, and kidney, were collected and excised to analyze the ex vivo fluorescence. In addition, healthy female BALB/c mice were also used to study the biodistribution of the prepared liposomes. Similarly, the mice were sacrificed 24 h post the injection, and the major tissues, including heart, liver, spleen, lung, kidney, and intestines, were collected and excised to analyze the ex vivo fluorescence.

To compare the pharmacokinetic profiles of PC-Lipo and PS-Lipo in mice, healthy BALB/c mice were intravenous injection wih DiD-labeled PC-Lipo or PS-Lipo at the same dose. Blood samples were collected from eye socket vein at 0.05 h, 0.5 h, 1 h, 2 h, 4 h, 8 h, 12 h, 24 h after injection, and centrifuged at 3000 rpm for 10 min. Plasma samples (20 μL) were added to 500 μL of methanol. Each sample was then centrifuged at 13 000 rpm for 5 min, and the supernatant was semi-quantified by a microplate reader. The fluorescence intensity at 0.05 h was set as 100% for normalization purposes.

In vivo biocompatibility

To study the in vivo biocompatibility of the prepared liposomes, healthy 8-week-old female BALB/c mice were randomized and divided into three groups ($n=5$). Then, the mice were treated by intravenous injection with saline, PC-Lipo, or PS-Lipo at the total lipid amount of 100 mg/kg body weight every 2 days. Two weeks later, the mice were sacrificed, and the blood was collected for hematological analysis. The red blood cells (RBC), white blood cells (WBC), hemoglobin level (HBL), alanine aminotransferase (ALT), aspartate aminotransferase (AST), and serum creatinine (CREA) were counted by a hemocytometer. In addition, the body weight of mice was also monitored to evaluate the systemic toxicity.

Histological analysis

Histological staining was carried out on the major tissues that were collected, including heart, liver, spleen, lung, kidney, intestine, and bone joints. The tissues were dehydrated using buffered formalin, ethanol, and xylene. Then, the samples were embedded in the liquid paraffin. The sliced samples (3–5 μm) were stained with H&E and examined by microscopy.

Statistical analysis

Data were presented as mean ± SD. Means were compared using one-way ANOVA followed by Student's t-test for two-sample comparison using GraphPad Prism v7.00. P values < 0.05 were considered statistically significant. $^{*}p<0.05$, $^{**}p<0.01$, $^{***}p<0.001$, $^{****}p<0.0001$.

Supplementary Information

The online version contains supplementary material available at https://doi.org/10.1186/s12951-024-02755-3.

Supplementary Material 1

Acknowledgements

We thank the staff members of Department of Diagnostic Radiology, Jinling Hospital, Nanjing Medical University, for providing technical support and assistance in data collection and analysis. Authors also extend acknowledgement to BioRender.com for creation of images.

Author contributions

QZ, LZ and HW designed the research. LZ, YJL, XL and XLH performed the experiments. JYZ, JZ, and YBQ analyzed the data. QZ, LZ, and FFS wrote the paper. All authors have reviewed the manuscript. All authors read and approved the final manuscript.

Funding

The work was supported by the National Natural Science Foundation of China (No. 81901890 to Qing Zhou and 82101063 to Li Zhang), the "3456" Cultivation Program for Junior Talents of Nanjing Stomatological School, Medical School of Nanjing University (No.0222R205 to Li Zhang), the Natural Science Foundation of Jiangsu Province (No. BK20200147 to Li Zhang), and the Innovation Capability Support Plan of Shaanxi Province (No. 2020TD-041 to Hong Wu).

Data availability

No datasets were generated or analysed during the current study.

Declarations

Ethics approval and consent to participate

All animal experiments were approved by the Animal Care and Use Committee of Nanjing University (IACUC-2003054) and under international regulations and standards on animal welfare.

Consent for publication

The authors confirm that the work described has not been published before, not under consideration for publication elsewhere. Its publication has been approved by all co-authors.

Competing interests

The authors declare no competing interests.

Received: 12 March 2024 / Accepted: 5 August 2024
Published online: 21 August 2024

References

1. Park MD, Silvin A, Ginhoux F, Merad M. Macrophages in health and disease. Cell. 2022;185(23):4259–79.
2. Varol C, Mildner A, Jung S. Macrophages: development and tissue specialization. Annu Rev Immunol. 2015;33:643–75.
3. Epelman S, Lavine KJ, Randolph GJ. Origin and functions of tissue macrophages. Immunity. 2014;41(1):21–35.
4. Perdiguero EG, Geissmann F. The development and maintenance of resident macrophages. Nat Immunol. 2016;17(1):2–8.
5. Nobs SP, Kopf M. Tissue-resident macrophages: guardians of organ homeostasis. Trends Immunol. 2021;42(6):495–507.
6. Cox N, Pokrovskii M, Vicario R, Geissmann F. Origins, biology, and diseases of tissue macrophages. Annu Rev Immunol. 2021;39:313–44.
7. Lazarov T, Juarez-Carreño S, Cox N, Geissmann F. Physiology and diseases of tissue-resident macrophages. Nature. 2023;618(7966):698–707.
8. Zhang C, Yan L, Wang X, Zhu S, Chen C, Gu Z, Zhao Y. Progress, challenges, and future of nanomedicine. Nano Today. 2020;35:101008.
9. Youn YS, Bae YH. Perspectives on the past, present, and future of cancer nanomedicine. Adv Drug Deliv Rev. 2018;130:3–11.
10. Albalawi F, Hussein MZ, Fakurazi S, Masarudin MJ. Engineered nanomaterials: the challenges and opportunities for nanomedicines. Int J Nanomed 2021:161–84.
11. Mitchell MJ, Billingsley MM, Haley RM, Wechsler ME, Peppas NA, Langer R. Engineering precision nanoparticles for drug delivery. Nat Rev Drug Discovery. 2021;20(2):101–24.
12. Martin C, Lowery D. mRNA vaccines: intellectual property landscape. Nat Rev Drug Discovery. 2020;19(9):578–9.
13. Szabó GT, Mahiny AJ, Vlatkovic I. COVID-19 mRNA vaccines: platforms and current developments. Mol Ther. 2022;30(5):1850–68.
14. Xiao Y, Shi J. Lipids and the emerging RNA medicines. Chem Rev. 2021;121(20):12109–11.
15. De Serrano LO, Burkhart DJ. Liposomal vaccine formulations as prophylactic agents: design considerations for modern vaccines. J Nanobiotechnol. 2017;15:1–23.
16. Allen TM, Cullis PR. Liposomal drug delivery systems: from concept to clinical applications. Adv Drug Deliv Rev. 2013;65(1):36–48.
17. Beltrán-Gracia E, López-Camacho A, Higuera-Ciapara I, Velázquez-Fernández JB, Vallejo-Cardona AA. Nanomedicine review: clinical developments in liposomal applications. Cancer Nanotechnol. 2019;10(1):1–40.
18. Segawa K, Nagata S. An apoptotic 'eat me'signal: phosphatidylserine exposure. Trends Cell Biol. 2015;25(11):639–50.
19. Naeini MB, Bianconi V, Pirro M, Sahebkar A. The role of phosphatidylserine recognition receptors in multiple biological functions. Cell Mol Biol Lett. 2020;25:1–17.
20. Kim O-H, Kang G-H, Hur J, Lee J, Jung Y, Hong I-S, Lee H, Seo S-Y, Lee DH, Lee CS. Externalized phosphatidylinositides on apoptotic cells are eat-me signals recognized by CD14. Cell Death Differ. 2022;29(7):1423–32.
21. Belhadj Z, He B, Deng H, Song S, Zhang H, Wang X, Dai W, Zhang Q. A combined eat me/don't eat me strategy based on extracellular vesicles for anticancer nanomedicine. J Extracell Vesicles. 2020;9(1):1806444.
22. Gan J, Dou Y, Li Y, Wang Z, Wang L, Liu S, Li Q, Yu H, Liu C, Han C. Producing anti-inflammatory macrophages by nanoparticle-triggered clustering of mannose receptors. Biomaterials. 2018;178:95–108.
23. Gao Q, Zhang J, Chen C, Chen M, Sun P, Du W, Zhang S, Liu Y, Zhang R, Bai M. In situ mannosylated nanotrinity-mediated macrophage remodeling combats Candida albicans infection. ACS Nano. 2020;14(4):3980–90.
24. Yang H, Zhu C, Yuan W, Wei X, Liu C, Huang J, Yuan M, Wu Y, Ling Q, Hoffmann PR. Mannose-rich oligosaccharides-functionalized selenium nanoparticles mediates macrophage reprogramming and inflammation resolution in ulcerative colitis. Chem Eng J. 2022;435:131715.
25. Rampado R, Peer D. Design of experiments in the optimization of nanoparticle-based drug delivery systems. J Controlled Release. 2023;358:398–419.
26. Luiz MT, Viegas JSR, Abriata JP, Viegas F, de Carvalho Vicentini FTM, Bentley MVLB, Chorilli M, Marchetti JM, Tapia-Blacido DR. Design of experiments (DoE) to develop and to optimize nanoparticles as drug delivery systems. Eur J Pharm Biopharm. 2021;165:127–48.
27. Zalba S, Ten Hagen TL, Burgui C, Garrido MJ. Stealth nanoparticles in oncology: facing the PEG dilemma. J Controlled Release. 2022;351:22–36.
28. Nakhaei P, Margiana R, Bokov DO, Abdelbasset WK, Jadidi Kouhbanani MA, Varma RS, Marofi F, Jarahian M, Beheshtkhoo N. Liposomes: structure, biomedical applications, and stability parameters with emphasis on cholesterol. Front Bioeng Biotechnol. 2021;9:705886.
29. Dugail I, Kayser BD, Lhomme M. Specific roles of phosphatidylglycerols in hosts and microbes. Biochimie. 2017;141:47–53.
30. Ngo W, Ahmed S, Blackadar C, Bussin B, Ji Q, Mladjenovic SM, Sepahi Z, Chan WC. Why nanoparticles prefer liver macrophage cell uptake in vivo. Adv Drug Deliv Rev. 2022;185:114238.
31. Deprez J, Verbeke R, Meulewaeter S, Aernout I, Dewitte H, Decruy T, Coudenys J, Van Duyse J, Van Isterdael G, Peer D. Transport by circulating myeloid cells drives liposomal accumulation in inflamed synovium. Nat Nanotechnol. 2023;18(11):1341–50.

32. Le ND, Nguyen BL, Patil BR, Chun H, Kim S, Nguyen TOO, Mishra S, Tandukar S, Chang J-H, Kim DY. Antiangiogenic therapeutic mRNA delivery using lung-selective polymeric nanomedicine for Lung Cancer Treatment. ACS Nano. 2024;18(11):8392–410.
33. Qiu M, Tang Y, Chen J, Muriph R, Ye Z, Huang C, Evans J, Henske EP, Xu Q. Lung-selective mRNA delivery of synthetic lipid nanoparticles for the treatment of pulmonary lymphangioleiomyomatosis. *Proceedings of the national academy of sciences* 2022, 119(8):e2116271119.
34. Cheng Q, Wei T, Farbiak L, Johnson LT, Dilliard SA, Siegwart DJ. Selective organ targeting (SORT) nanoparticles for tissue-specific mRNA delivery and CRISPR–Cas gene editing. Nat Nanotechnol. 2020;15(4):313–20.
35. Sun Y, Chatterjee S, Lian X, Traylor Z, Sattiraju SR, Xiao Y, Dilliard SA, Sung Y-C, Kim M, Lee SM. In vivo editing of lung stem cells for durable gene correction in mice. Science. 2024;384(6701):1196–202.
36. Shah S, Dhawan V, Holm R, Nagarsenker MS, Perrie Y. Liposomes: advancements and innovation in the manufacturing process. Adv Drug Deliv Rev. 2020;154:102–22.
37. Filipczak N, Pan J, Yalamarty SSK, Torchilin VP. Recent advancements in liposome technology. Adv Drug Deliv Rev. 2020;156:4–22.
38. Chassaing B, Aitken JD, Malleshappa M, Vijay-Kumar M. Dextran sulfate sodium (DSS)-induced colitis in mice. Curr Protocols Immunol. 2014;104(1):15. 11-15.25. 14.
39. Raviv SA, Alyan M, Egorov E, Zano A, Harush MY, Pieters C, Korach-Rechtman H, Saadya A, Kaneti G, Nudelman I. Lung targeted liposomes for treating ARDS. J Controlled Release. 2022;346:421–33.
40. Yan F, Zhong Z, Wang Y, Feng Y, Mei Z, Li H, Chen X, Cai L, Li C. Exosome-based biomimetic nanoparticles targeted to inflamed joints for enhanced treatment of rheumatoid arthritis. J Nanobiotechnol. 2020;18:1–15.

Publisher's Note